

Testing Modified Newtonian dynamics through statistics of velocity dispersion profiles in the inner regions of elliptical galaxies

Kyu-Hyun Chae^{1*} and In-Taek Gong¹

¹*Department of Physics and Astronomy, Sejong University, 98 Gunja-dong, Gwangjin-Gu, Seoul 143-747, Republic of Korea*

**chae@sejong.ac.kr*

Accepted; Received; in original form

ABSTRACT

Modified Newtonian dynamics (MOND) proposed by Milgrom provides a paradigm alternative to dark matter (DM) that has been successful in fitting and predicting the rich phenomenology of rotating disc galaxies. There have also been attempts to test MOND in dispersion-supported spheroidal early-type galaxies, but it remains unclear whether MOND can fit the various empirical properties of early-type galaxies for the whole ranges of mass and radius. As a way of rigorously testing MOND in elliptical galaxies we calculate the MOND-predicted velocity dispersion profiles (VDPs) in the inner regions of ~ 2000 nearly round SDSS elliptical galaxies under a variety of assumptions on velocity dispersion (VD) anisotropy, and then compare the predicted distribution of VDP slopes with the observed distribution in 11 ATLAS^{3D} galaxies selected with essentially the same criteria. We find that the MOND model parameterised with an interpolating function that works well for rotating galaxies can also reproduce the observed distribution of VDP slopes based only on the observed stellar mass distribution without DM or any other galaxy-to-galaxy varying factor. This is remarkable in view that Newtonian dynamics with DM requires a specific amount and/or profile of DM for each galaxy in order to reproduce the observed distribution of VDP slopes. When we analyse non-round galaxy samples using the MOND-based spherical Jeans equation, we do not find any systematic difference in the mean property of the VDP slope distribution compared with the nearly round sample. However, in line with previous studies of MOND through individual analyses of elliptical galaxies, varying MOND interpolating function or VD anisotropy can lead to systematic change in the VDP slope distribution, indicating that a statistical analysis of VDPs can be used to constrain specific MOND models with an accurate measurement of VDP slopes or a prior constraint on VD anisotropy.

Key words: dark matter – galaxies: elliptical and lenticular, cD – galaxies: kinematics and dynamics – galaxies: structure – gravitation

1 INTRODUCTION

Mass discrepancy (or missing mass) problems in galaxies, galaxy clusters and the Universe have usually been attributed to dark matter (DM) assuming that standard Newton-Einstein gravity is valid in those dynamical systems (for reviews, see, e.g., Trimble 1987; Bertone, Hooper & Silk 2005; Sanders 2014a). The currently popular Lambda cold dark matter (Λ CDM) cosmological paradigm of the Universe provides a successful phenomenological model of the large-scale structure, the cosmological microwave background radiation (CMBR) anisotropy power spectrum, and the expansion history of the Universe (e.g.

Hinshaw et al. 2013; Ade et al. 2014). Theories of galaxy formation and evolution based on the Λ CDM paradigm have also been making progress with the goal of explaining the rich phenomenology of galaxies (for a review see, e.g., Mo, van den Bosch & White 2010).

However, in the realm (where dynamics is non-linear) of galaxies the Λ CDM paradigm appears to face serious challenges. Rotation curves of disc galaxies start to deviate from Newtonian expectation all at the same critical acceleration scale $a_0 \approx 1.2 \times 10^{-10} \text{ m s}^{-2}$ regardless of galaxy size, luminosity, surface brightness or any other property (McGaugh 2004; Famaey & McGaugh 2012). The velocity at the flat

part of the rotation curve is well correlated with the total baryonic mass of the galaxy (consistent with zero intrinsic scatter) spanning five orders-of-magnitude in baryonic mass from giant spiral galaxies to low surface brightness galaxies; this correlation is now known as the baryonic Tully-Fisher relation (McGaugh 2005, 2011; Famaey & McGaugh 2012). Furthermore, to every feature in an individual rotation curve there corresponds a feature in baryonic mass density profile even in galaxies whose dynamics should be dominated by DM if the Λ CDM paradigm is assumed (Sancisi 2004; Famaey & McGaugh 2012).

The apparent existence of the critical acceleration a_0 and the intimate connection between the galaxy rotation curve and the baryonic mass distribution seems unnatural in the Λ CDM paradigm. Other outstanding challenges of the Λ CDM paradigm in galaxies such as the number and distribution of DM subhaloes and the DM central cusp/core density profile are also well documented in the literature (Famaey & McGaugh 2012; Kroupa, Pawlowski & Milgrom 2012; McGaugh 2014).

Milgrom's modified Newtonian dynamics (MOND; Milgrom 1983) offers an alternative paradigm that can bypass the above challenges of rotating galaxies faced by the Λ CDM paradigm. The MOND paradigm posits that Newton's law of gravity breaks down at extremely low accelerations below the critical acceleration a_0 . Then, the phenomenological existence of a_0 , the baryonic Tully-Fisher relation, and so on can be unified in a single MOND law (see Famaey & McGaugh 2012 for an extensive review). Whether the empirical MOND law can be ultimately explained by a fundamental law of modified gravity or somehow by revised theories of galaxy formation under the Λ CDM paradigm, it is clearly worthwhile as a Kepler-like law of galactic kinematics. If the remarkable success of the MOND paradigm in rotating galaxies implies an underlying law, it must also explain the empirical properties of spheroidal early-type (elliptical and lenticular) galaxies (ETGs) that are different from disc galaxies in dynamics and structure. In this respect it is quite interesting to test MOND in ETGs.

However, testing MOND (or DM) in ETGs is far more challenging because they lack neutral hydrogens (the crucial dynamical tracer for disc galaxies) and orbits of stars (and other tracers) are complex (and/or unknown). Nevertheless, significant efforts have been made to test MOND (and DM) in ETGs using dynamical tracers such as stars, planetary nebulae (PNe), globular clusters (GCs), hot X-ray gases, satellite galaxies, and gravitational lensing. Despite significant efforts, it is not yet clear whether MOND can provide a successful phenomenological model for the dynamics of ETGs. Sometimes, analyses of the same galaxies often reached different conclusions.

Based on the kinematics of PNe (out to $\sim 5R_e$ where R_e is the effective radius) of three elliptical galaxies, Milgrom & Sanders (2003) argued that MOND could explain the observed kinematics well and no DM would be needed. However, for the same galaxies Dekel et al. (2005) argued that DM would be consistent with the data once radially varying velocity dispersion (VD) anisotropies were allowed. Independent analyses of PNe kinematics of two other ellipticals by Tirit et al. (2007) and Samurović (2010) showed that MOND could explain the kinematics without DM. Based on the velocity dispersion profiles (VDPs) of

stacked SDSS satellite galaxies around two narrow luminosity ranges of red galaxies Klypin & Prada (2009) and Angus et al. (2008) reached opposite conclusions respectively against and for MOND because of their different assumptions on the profiles of density and VD anisotropy of satellites. Milgrom (2012) tested MOND using the mass profiles of two X-ray bright elliptical galaxies deduced assuming hydrostatic equilibrium and found that MOND successfully reproduced the profiles over a wide acceleration range from $> 10a_0$ (near the galactic centre) down to $\sim 0.1a_0$ (over 100-200 kpc). Analyses of (the masses of) strong lens ETGs also produced confusing results, some arguing against MOND (e.g. Ferreras et al. 2012) while others for MOND (e.g. Chiu et al. 2011; Sanders 2014b).

Based on the kinematics of GCs (out to several R_e) several studies (Samurović & Ćirković 2008; Richtler et al. 2008; Schubert et al. 2012; Samurović 2012, 2014) tested MOND in a handful of elliptical galaxies. In particular, Samurović (2014) carried out a systematic analysis of ten elliptical galaxies covering a broad range of mass. These studies of GC kinematics employed spherical Jeans analyses assuming isotropy or relatively simple anisotropies. According to these studies, as Samurović (2014) emphasized, MOND alone without an additional DM component could not provide a successful fit for several massive slow rotators in their outer regions (beyond $\sim 3R_e$), although MOND was generally successful for less massive fast rotators (where the slow/fast dichotomy is in the sense by Emsellem et al. 2007). Richtler et al. (2008) also advocated the need of DM under MOND in the central massive galaxy of the Fornax cluster. It is unclear whether these results imply the breakdown of MOND for a class of elliptical galaxies. The main limits of these studies are small sample sizes and uncertainties in VD anisotropy.

A rigorous test of MOND in ETGs would require (1) a statistically representative sample of ETGs and (2) an empirical probe of mass profile over a wide acceleration range. Here, we propose a test of MOND in elliptical galaxies satisfying the first requirement to a large extent and the second requirement only partially. We calculate MOND-based VDPs of ~ 2000 nearly round galaxies from Chae, Bernardi & Kravtsov (2014) for $0.1R_e < r < R_e$ using the observed stellar mass distributions under a variety of possibilities of VD anisotropy. We calculate the slopes of the VDPs for $0.1R_e < r < R_e$ and compare the distribution of the slopes with the measured distribution in a similarly selected sample of 11 nearly round ATLAS^{3D} (Cappellari et al. 2011) galaxies. Hence our analysis is statistical in nature. We describe the data and the method of analysis in section 2 and the results in section 3. We discuss implications of our results for MOND and give our conclusions in section 4.

2 DATA AND METHOD OF ANALYSIS

We consider only elliptical galaxies that are nearly round so that they can be analysed based on the spherical symmetry assumption with minimal error. A statistically representative sample of nearly round galaxies can be drawn from the immense Sloan Digital Sky Survey (SDSS; York et al. 2000)

data base.¹ We use a sample of SDSS galaxies defined and analysed under the Λ CDM paradigm by Chae et al. (2014) (see also Bernardi et al. 2010) that contains photometric parameters recently investigated and measured by Meert et al. (2013) and Meert et al. (2015) based on data release (DR) 7 data.² The sample contains 2054 elliptical galaxies with a mean redshift of $\langle z \rangle \approx 0.12$ spanning two orders of magnitude in stellar mass that are nearly round (projected minor-to-major axis ratio $b/a > 0.85$) and do not possess a measurable disc.

Because each galaxy has no measurable disc by selection, its light distribution on the sky can be well-described by a Sérsic (1968) profile

$$\Sigma(R) \propto \exp \left[-b_{n_{\text{Ser}}} \left(\frac{R}{R_e} \right)^{1/n_{\text{Ser}}} \right], \quad (1)$$

where n_{Ser} is referred to as Sérsic index and $b_{n_{\text{Ser}}} = 2n_{\text{Ser}} - 1/3 + 0.009876/n_{\text{Ser}}$ (Prugniel & Simien 1997). Deprojecting equation (1) we obtain a volume luminosity density profile $\rho(r)$ and then a stellar mass density profile through a stellar initial mass function (IMF). (For our selected galaxies gas is ignorable particularly because they do not possess a measurable disc.) Each galaxy has also a measured VD σ_{ap} within the SDSS aperture of $R_{\text{ap}} = 1.5$ arcsec radius which corresponds to a physical radius between $0.1R_e$ and R_e with a mean of $\langle R_{\text{ap}}/R_e \rangle \approx 0.5$. Note that σ_{ap} denotes a luminosity-weighted average of line-of-sight velocity dispersions (LOSVDs) of all stars within the aperture.

Under the standard Newtonian dynamics the observed VD σ_{ap} may be reproduced by adjusting the stellar mass-to-light (M_*/L) ratio or equivalently the stellar IMF for a flexible assumption of DM mass profile (even including the case of no DM) given the empirical intrinsic galaxy-to-galaxy scatter of IMF. This means that σ_{ap} (an average quantity within a region) itself may not be a sensitive probe of gravity or mass distribution. However, the VDP is a powerful probe. The observed VDP of an individual galaxy over a radial range can be used to infer the total mass profile for that range under Newtonian dynamics (e.g. Thomas et al. 2007). For a large sample of galaxies that do not have individually measured VDPs one can, as done in Chae et al. (2014), predict VDPs using galaxy models satisfying the available observational constraints, and then compare the statistical distribution of VDPs with an available empirical distribution. Such a comparison of VDP slope distributions clearly shows that galaxies must be embedded in DM halos to match the empirical distribution if Newtonian dynamics is assumed to be valid at all acceleration scale (see Chae et al. 2014 and below).

Here we carry out a similar statistical analysis of VDP slopes under MOND. Our analysis is based on the spherical Jeans equation given in MOND (e.g. Angus et al. 2008; Klypin & Prada 2009) by

$$\frac{d[\rho(r)\sigma_r^2(r)]}{dr} + 2\frac{\beta(r)}{r}[\rho(r)\sigma_r^2(r)] = -\rho(r)g(r), \quad (2)$$

where $\rho(r)$ is the volume luminosity density at radius r , $\sigma_r(r)$ is the radial stellar VD, and $\beta(r)$ is the VD anisotropy given by $\beta(r) = 1 - \sigma_t^2(r)/\sigma_r^2(r)$ where $\sigma_t(r)$ is the tangential VD in spherical coordinates. In equation (2) $g(r)$ is the MONDian (‘effective’ or ‘real’) gravitational acceleration which differs from the Newtonian acceleration $g_N(r) = GM_b(r)/r^2$ for the baryonic (stellar here) mass $M_b(r)$ within r . The acceleration g approaches g_N for $g/a_0 \gg 1$ but tends to $\sqrt{g_N a_0}$ as $g/a_0 \rightarrow 0$ (hence $g(r)$ due to a point mass makes a transition from the Newtonian inverse square law $g(r) \propto r^{-2}$ for $g/a_0 \gg 1$ to $g(r) \propto r^{-1}$ for $g/a_0 \ll 1$). The transition between the Newtonian and the MONDian regimes is parameterised by

$$g_N = \mu(g/a_0)g \quad (3)$$

where interpolating function $\mu(x)$ satisfies $\mu(x) \rightarrow 1$ for $x \gg 1$ and $\mu(x) \rightarrow x$ for $x \ll 1$. The transition can also be written as the inverted relation

$$g = \nu(g_N/a_0)g_N, \quad (4)$$

where $\nu(y)$ satisfies $\nu(y) \rightarrow 1$ for $y \gg 1$ and $\nu(y) \rightarrow y^{-1/2}$ for $y \ll 1$.

We consider a class of interpolating functions given by

$$\mu_n(x) = \frac{x}{(1+x^n)^{1/n}} \quad (5)$$

with the corresponding inverted function (Milgrom & Sanders 2008)

$$\nu_n(y) = \left[\frac{1 + (1 + 4y^{-n})^{1/2}}{2} \right]^{1/n}, \quad (6)$$

where the case $n = 2$ is traditionally known as the ‘standard’ function while the ‘simple’ case $n = 1$ introduced by Famaey & Binney (2005) has turned out performing well in various recent studies (e.g. Sanders & Noordermeer 2007; Angus et al. 2008; Milgrom 2012). We also consider the interpolating function implied by Bekenstein’s relativistic theory of modified gravity given by (Bekenstein 2004; Zhao & Famaey 2006)

$$\mu_{\text{Bek}}(x) = \frac{\sqrt{1+4x} - 1}{\sqrt{1+4x} + 1} \quad (7)$$

with the corresponding inverted function

$$\nu_{\text{Bek}}(y) = 1 + y^{-1/2}. \quad (8)$$

For MONDian dynamical analyses of a galaxy any external field in which the galaxy is embedded should, in principle, be taken into account. A MONDian external field effect (EFE; Milgrom 1983; Famaey, Bruneton & Zhao 2007; Richtler et al. 2011) may particularly matter for those in the central regions of galaxy clusters and those having close neighbors. Most galaxies in our SDSS sample are not in cluster centres and have light distributions “uncontaminated” by neighbors. Also, an evaluation of EFEs for elliptical galaxies using the Virgo and Coma clusters by Richtler et al. (2011) indicates that the expected effects are small. In this work we do not consider including EFEs for our selected galaxies.

For a given baryonic mass profile $M_b(r)$ with the corresponding luminosity density $\rho(r)$ the solution of equation (2) for the radial stellar VD $\sigma_r(r)$ can be given following appendix B of Chae et al. (2012) as

¹ <http://www.sdss.org/>

² The Meert et al. (2015) photometric measurements for full DR7 data can be downloaded at http://shalaowai.physics.upenn.edu/~ameert/fit_catalog/download/

$$\sigma_r^2(r) = G \int_r^\infty \frac{\omega(t)}{\omega(r)} \frac{\rho(t)}{\rho(r)} \frac{M_b(t)}{t^2} \nu \left(\frac{G}{a_0} \frac{M_b(t)}{t^2} \right) dt, \quad (9)$$

where $\omega(r) = \exp \left[\int^r (2\beta(r')/r') dr' \right]$ for an anisotropy $\beta(r')$ and $\nu(y)$ is an inverted interpolating function. The LOSVD of stars at projected radius R on the sky is then given by (e.g. Binney & Mamon 1982)

$$\sigma_{\text{los}}^2(R) = \frac{1}{\Sigma(R)} \int_{R^2}^\infty \rho(r) \sigma_r^2(r) \left[1 - \frac{R^2}{r^2} \beta(r) \right] \frac{dr^2}{\sqrt{r^2 - R^2}}, \quad (10)$$

where $\Sigma(R)$ is given by equation (1). The luminosity weighted LOSVD within projected radius R is given as

$$\sigma(R) \equiv \langle \sigma_{\text{los}} \rangle(R) = \frac{\int_0^R \Sigma(R') \sigma_{\text{los}}(R') R' dR'}{\int_0^R \Sigma(R') R' dR'}, \quad (11)$$

and thus the aperture VD is $\sigma_{\text{ap}} = \sigma(R = R_{\text{ap}})$.

Three factors can be involved in the connection between the observationally derived luminosity density $\rho(r)$ and the observed VD σ_{ap} : the stellar mass-to-light ratio M_*/L , the VD anisotropy profile $\beta(r)$ and the (inverted) interpolating function $\nu(g_N(r)/a_0)$. Bernardi et al. (2010) provide stellar masses (or stellar mass-to-light ratios) of SDSS ETGs based on the Chabrier (2003) IMF. Following the literature (e.g. Chae et al. 2014) we define a stellar mass-to-light ratio or IMF mismatch parameter

$$\delta_M \equiv \log_{10}(M_*/M_{\star}^{\text{Ch}}) = \log_{10} \left[\frac{(M_*/L)}{(M_*/L)^{\text{Ch}}} \right] \quad (12)$$

between the unknown stellar mass M_* (or M_*/L) and the fiducial stellar mass M_{\star}^{Ch} [or $(M_*/L)^{\text{Ch}}$] derived by Bernardi et al. (2010) based on the Chabrier (2003) IMF. All the uncertainties related to photometric measurement, mass-to-light ratio, and/or IMF are then absorbed into this single parameter δ_M . Since our goal is to test MOND i.e. its interpolating functions, we need empirical inputs or assumptions for δ_M and $\beta(r)$.³ Here we take an approach similar to Chae et al. (2014). The empirical input for δ_M is provided by the literature results on VD-dependent stellar IMF (e.g. Cappellari et al. 2013b; Conroy & van Dokkum 2012; Tortora, Romanowsky & Napolitano 2013; see below). For $\beta(r)$ we consider both constant β and double Osipkov-Merritt-type (Chae et al. 2012; Chae 2014) $\beta_{\text{dOM}}(r) = \beta_1/(1+r_1^2/r^2) + \beta_2/(1+r_2^2/r^2)$, where $\beta_1 + \beta_2 = \beta(r \rightarrow \infty) \equiv \beta_\infty$. For constant β each value is drawn from a Gaussian distribution. For $\beta_{\text{dOM}}(r)$ the radial mean for $0 \leq r \leq R_e$, referred to as β_e ,⁴ and the value at infinity (β_∞) are drawn from a Gaussian distribution and r_1 and r_2 are randomly assigned satisfying $0 < r_1/R_e < r_2/R_e < 1$. The adopted function $\beta_{\text{dOM}}(r)$ is intended to encompass (not exhaustively) possible behaviours of anisotropy.

For input distributions of δ_M and $\beta(r)$ (constant or double Osipkov-Merritt-type) we search randomly for a pair reproducing σ_{ap} within a typical measurement error of 0.04 dex for the observationally derived $\rho(r)$ of each galaxy. For most galaxies a pair is easily found. For a few per cent of

³ If a VDP is measured for a radial range of a galaxy, then one can in principle simultaneously solve for δ_M and $\beta(r)$ for that range for the measured $\rho(r)$ and $\sigma(R)$.

⁴ The relation between (β_e, β_∞) and (β_1, β_2) can be found in appendix B of Chae et al. (2014)

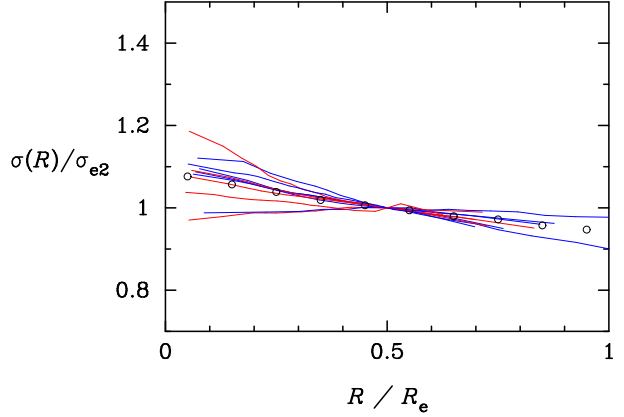


Figure 1. Profiles of luminosity-weighted LOSVD $\sigma(R)$ (equation 11) for 11 nearly round ATLAS^{3D} galaxies for which LOSVDs have been measured over 300 bins in the optical region (see the text). Red and blue profiles represent respectively slow and fast rotators. The abscissa is radius R on the sky normalized by the effective radius R_e while the ordinate is normalized by $\sigma_{e2} \equiv \sigma(R = R_e/2)$. Small circles represent the mean of the displayed profiles.

galaxies a successful pair could not be found after a significant number of trials. For each successful model we calculate a VDP $\sigma(R)$ (equation 11) as a function of radius R on the plane of the sky. We use a power-law approximation

$$\frac{\sigma(R)}{\sigma_{e2}} = \left(\frac{R}{R_e/2} \right)^\eta \quad (13)$$

for $0.1R_e < R < R_e$, where $\sigma_{e2} \equiv \sigma(R = R_e/2)$ and the value of η for each model is determined through a least-square fit. The statistical distribution of η for the galaxy models is then compared with an empirical distribution.

Published values of η for dozens of ETGs have a mean of $\langle \eta \rangle = -0.06 \pm 0.01$ with a galaxy-to-galaxy intrinsic scatter of $\sigma_\eta = 0.03 - 0.04$ (e.g. Chae et al. 2014; Cappellari et al. 2006). For a more reliable comparison with our nearly round galaxies we select galaxies from the ATLAS^{3D} (Cappellari et al. 2011) public data⁵ using the same criteria. Out of 260 ATLAS^{3D} ETGs 33 galaxies satisfy projected $b/a > 0.85$ in both photometric (Cappellari et al. 2013a) and kinematic (Emsellem et al. 2011) distributions within both $R_e/2$ and R_e . Seventeen of them are elliptical and out of these fifteen have measured values of LOSVD over 300 bins (pixels) on the plane of the optical region allowing reliable measurement of η . Finally, excluding galaxies having the mean of bulge and total Sérsic indices $n_{\text{Ser}} < 2.5$ as for the SDSS ETG sample (Chae et al. 2014) we are left with 11 galaxies: they are NGC 3193, 3379, 4168, 4278, 4283, 4374, 4458, 4552, 5173, 5638, and 5846. For each galaxy about 20 concentric rings are defined within R_e . LOSVDs of the bins in each ring are averaged and weighted with the surface brightness (Scott et al. 2013) of the ring and then these luminosity-weighted average LOSVDs give a $\sigma(R)$ profile. The derived $\sigma(R)$ profiles for the 11 galax-

⁵ <http://www-astro.physics.ox.ac.uk/atlas3d/>

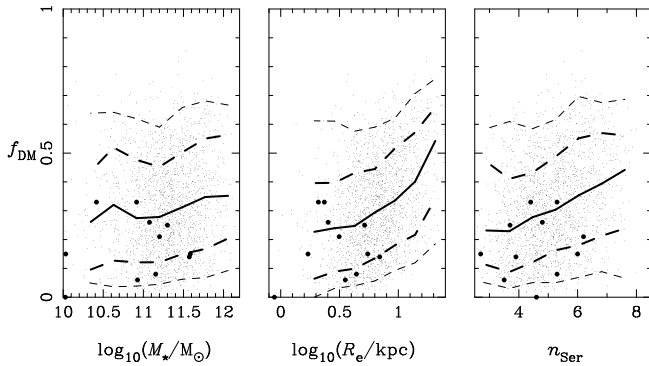


Figure 2. Dark matter fraction within the sphere of radius equal to R_e (f_{DM}) in SDSS and ATLAS^{3D} nearly round galaxies as a function of stellar mass (M_*), effective radius (R_e) and Sérsic index (n_{Ser}). Large dots represent 11 ATLAS^{3D} galaxies. SDSS galaxies are represented by small dots with thick solid curves representing the median values, thick and thin dashed curves the 68% and 95% limits respectively. See the text for details.

ies are displayed in Fig. 1. For these galaxies the least-square fit power-law slopes for $0.1R_e < R < R_e$ have a mean of $\langle \eta \rangle = -0.057 \pm 0.011$ with a standard deviation of 0.037 ± 0.007 (where the quoted errors have been estimated from bootstrap resampling) consistent with published results for ETGs of any ellipticity (Chae et al. 2014; Cappellari et al. 2006).

Emsellem et al. (2011) classify ATLAS^{3D} ETGs by the degree of large-scale rotation using the criterion defined by Emsellem et al. (2007). As noted in section 1, some previous tests (based mostly on GC kinematics) of MOND in elliptical galaxies obtained contrasting results for fast and slow rotators [MOND was not successful for the outer part ($\gtrsim 2-3R_e$) kinematics of slow rotators in several cases; see Samurović (2014) and references therein]. For SDSS ETGs this kinematic information is missing. The majority (86 ± 2 per cent) of ATLAS^{3D} ETGs are classified as fast rotators. However, for the above 11 ATLAS^{3D} ellipticals selected using essentially the same criteria as for the SDSS sample, about one half (6 out of 11) are fast rotators. These two kinematic classes of galaxies have mean VDP slopes $\langle \eta \rangle = -0.067 \pm 0.014$ (fast) versus -0.046 ± 0.017 (slow) where the discrepancy is not statistically significant based on the small samples. We caution, however, that the low precision of current samples does not allow a sensitive test.

Fig. 2 shows the distributions of dark matter fraction within the effective radius (f_{DM}) for the SDSS and the ATLAS^{3D} nearly round galaxies as a function of stellar mass (M_*), effective radius (R_e) and Sérsic index (n_{Ser}), where SDSS parameter values are taken from the Chae et al. (2014) modelling result for their fiducial inputs. There are significant differences between SDSS and ATLAS^{3D} samples. SDSS galaxies have larger f_{DM} overall (mean $\langle f_{\text{DM}} \rangle \approx 0.32$ versus 0.18) and are biased towards greater stellar masses (mean $\log_{10}(M_*/M_\odot) \approx 11.3$ versus 10.8) and (more noticeably) larger sizes (mean $\log_{10}(R_e/\text{kpc}) \approx 0.82$ versus 0.48). The range of modelling results considered by Chae et al. (2014) taking into account various systematic effects give $0.27 \lesssim f_{\text{DM}} \lesssim 0.38$. The second panel of Fig. 2 indicates that

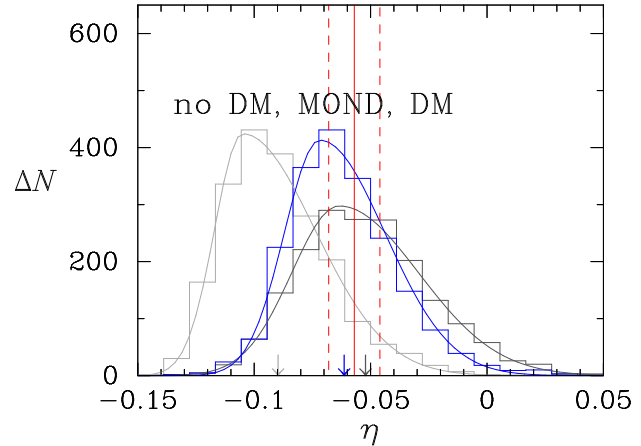


Figure 3. Predicted distributions of VDP slope η (equation 13) for ~ 2000 nearly round SDSS elliptical galaxies. Three cases are compared: Newtonian cases without and with DM presented in Chae et al. (2014) and a MOND case calculated here for $(n, \langle \beta \rangle) = (1.5, 0)$ and shown in Fig. 4. Vertical red solid and dashed lines indicate the measured mean and its error for 11 ATLAS^{3D} nearly round galaxies shown in Fig. 1. The arrows indicate the mean values of the distributions.

the difference in $\langle f_{\text{DM}} \rangle$ can be in large part attributed to the difference in galaxy sizes. Indeed, at $\log_{10}(R_e/\text{kpc}) = 0.5$ SDSS galaxies have $f_{\text{DM}} \approx 0.25$ (with a systematic error of ~ 0.05 due to input variations) getting closer to 0.18 of ATLAS^{3D} galaxies.

The difference in R_e between the SDSS and the ATLAS^{3D} samples may be due to various factors including different parent populations, measurement errors and different methods of modelling light profiles. The ATLAS^{3D} parent sample is a volume limited sample in the local Universe within $D < 42$ Mpc (almost) complete for $M_* \gtrsim 6 \times 10^9 M_\odot$ (Cappellari et al. 2011). The SDSS parent sample is magnitude-limited to cosmological distances (up to redshift ~ 0.2 with a median redshift of ~ 0.1) and thus completeness becomes less secure for less luminous galaxies and at larger distances. It is also likely that measurement/modelling errors are at work as can be seen, e.g., from the systematic difference between RC3 and 2MASS photometric data for the same ATLAS^{3D} galaxies (Cappellari et al. 2011) and dependence on modelling details for SDSS galaxies (Meert et al. 2013).

We assume that the statistical distribution of η is not significantly affected by such sample difference as that between SDSS and ATLAS^{3D} samples and use the measured distribution of η for the ATLAS^{3D} galaxies to interpret modelling results for the SDSS galaxies. We also make no distinction between fast and slow rotators and note that our selected ATLAS^{3D} galaxies are nearly evenly divided (Fig. 1).

3 RESULTS

The output distribution of η for the SDSS galaxy sample can depend on the input stellar IMF (distribution), parameterised by δ_M (equation 12), and VD anisotropy $\beta(r)$ for a given MOND model (interpolating function).

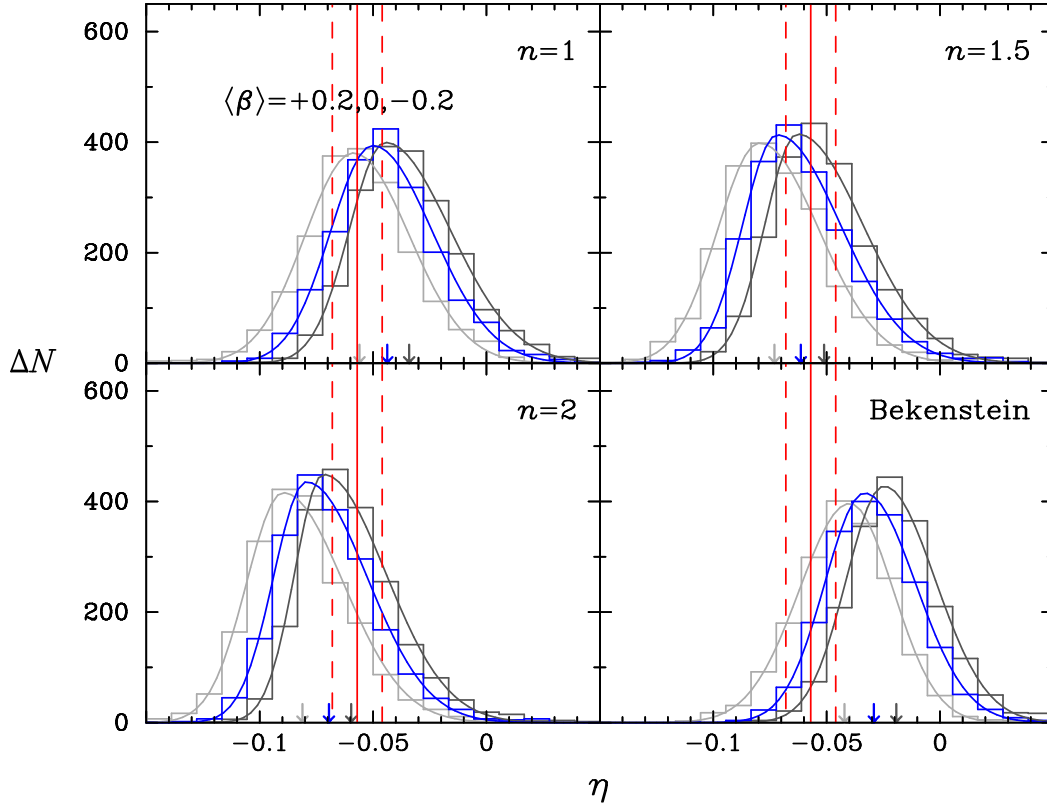


Figure 4. Predicted distribution of VDP slope η (equation 13) for the SDSS galaxy sample depending on MOND interpolation function and VD anisotropy mean value $\langle\beta\rangle$ assuming anisotropy is constant and has a galaxy-to-galaxy scatter of 0.2. We consider a MOND interpolation function of the form given by equation (5) with index $n = 1, 1.5$ and 2 as well as that given by equation (7) taken from Bekenstein’s (2004) relativistic theory of modified gravity. For each MOND model we consider three cases of $\langle\beta\rangle = +0.2$ (light gray), $\langle\beta\rangle = 0$ (blue) and $\langle\beta\rangle = -0.2$ (dark gray). Red lines are the same as in Fig. 3. The arrows indicate the mean values of the distributions.

Our standard choice for the VD-dependent stellar IMF is that preferred by ATLAS^{3D} (Cappellari et al. 2013b), which can be re-expressed in our adaptation as $\delta_M = 0.11 + 0.35 \log_{10}(2^{-0.06} \sigma_{e2}/130 \text{ km s}^{-1})$. Unless specified otherwise, all presented results are based on the input of this ATLAS^{3D} IMF distribution. However, as demonstrated below, it turns out that the output η distribution is only weakly dependent on the input δ_M distribution.

We first compare the Newtonian cases without and with DM presented in Chae et al. (2014) with a MOND case. The results for the three cases are shown in Fig. 3. The Newtonian case with DM reproduced here is the result based on the fiducial inputs by Chae et al. (2014). Newtonian dynamics clearly requires DM in a statistical sense (see also Fig. 2) and can match the observed VDP distribution with adjustment of various inputs (Chae et al. 2014). However, it is also evident that MOND can reproduce well the VDP distribution.

We present in turn MOND results for constant anisotropy (section 3.1) and for varying anisotropy of the form $\beta_{\text{dOM}}(r)$ (section 3.2).

3.1 Constant anisotropy

Anisotropy values are drawn from a Gaussian distribution with a mean of $\langle\beta\rangle$ and a standard deviation of 0.2, which is motivated from studies of nearby early-type galaxies (e.g. Gerhard et al. 2001; Cappellari et al. 2007; Thomas et al. 2007). The predicted distribution of η for the SDSS galaxy sample then depends on the input mean anisotropy $\langle\beta\rangle$ and MOND interpolating function. We consider $\langle\beta\rangle = +0.2$ (light gray), 0 (blue), and -0.2 (dark gray) for each of $n = 1, 1.5$, and 2 in the function given by equation (5) as well as for the function given by equation (7). The results are displayed in Fig. 4. For $n = 1.5$ the predicted mean of η can match easily the measured value. The cases $n = 1$ and $n = 2$ can also match the measured distribution but not for all the cases of $\langle\beta\rangle$. The case $n = 1$ prefers $\langle\beta\rangle = +0.2$ while $n = 2$ prefers $\langle\beta\rangle = -0.2$. These results imply that a number of degenerate sets of $(n, \langle\beta\rangle)$ can be consistent with the measured η value. However, Bekenstein’s model is disfavoured for the assumed cases of constant anisotropies.

In our approach it turns out that the output distribution of η is only weakly dependent on the input IMF. In the random process of finding (δ_M, β) where δ_M (equation 12) is essentially a representation of the stellar mass-to-light ratio depending on the IMF, the posterior distribution of δ_M generally deviates from the prior

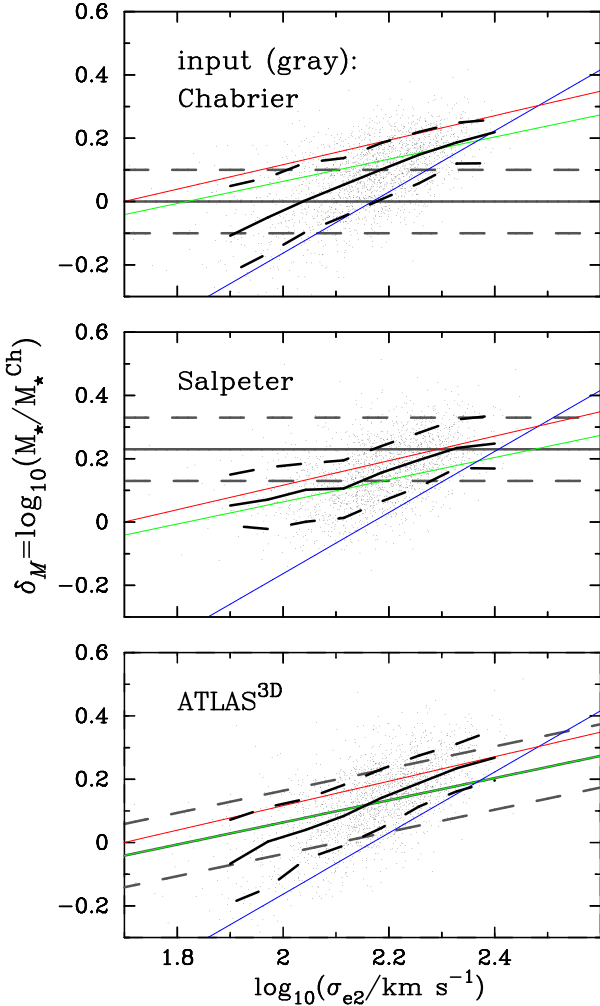


Figure 5. Input and output distributions of stellar IMF mismatch parameter δ_M (equation 12). Three input IMFs are represented by gray lines with an intrinsic scatter of 0.1 dex (represented by dashed lines): Chabrier (2003), Salpeter (1955) and ATLAS^{3D} (Cappellari et al. 2013b). Data points are the output models and the black lines indicate the median relations (with dashed lines indicating the 68 percent limits). Thin lines represent recently measured IMF behaviours: red – Conroy & van Dokkum (2012); green – Cappellari et al. (2013b); blue – Tortora et al. (2013).

input distribution. Fig. 5 shows the distributions of δ_M for three cases of input IMF: two VD-independent cases of Chabrier (2003) and Salpeter (1955) and one VD-dependent case of ATLAS^{3D} (Cappellari et al. 2013b), with an intrinsic scatter of 0.1 dex (Cappellari et al. 2013b) imposed in all cases. Irrespective of the input IMF the posterior mean of δ_M increases with VD and its functional behaviour is well within the behaviours of recently inferred IMFs (Conroy & van Dokkum 2012; Cappellari et al. 2013b; Tortora, Romanowsky & Napolitano 2013).

For the cases of constant anisotropy the predicted width (containing 68 percent of galaxies) and standard deviation of η (~ 0.23) are smaller than the measured standard deviation of $\sigma_\eta \approx 0.037 \pm 0.007$. This discrepancy is largely removed if varying anisotropies are used as described in section 3.2.

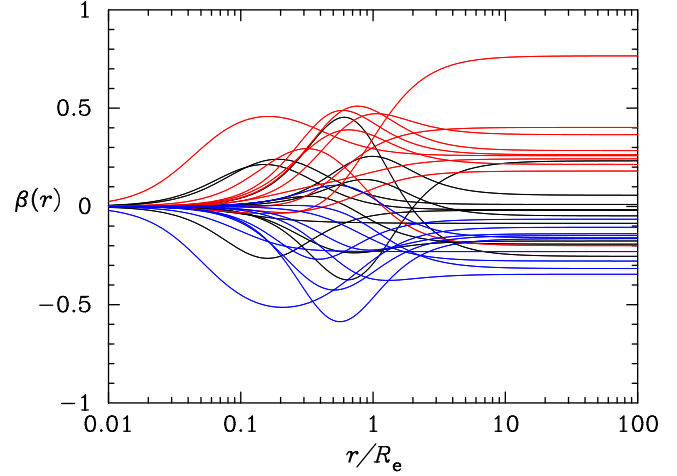


Figure 6. Examples of varying anisotropy $\beta_{\text{dOM}}(r) = \beta_1/(1 + r_1^2/r^2) + \beta_2/(1 + r_2^2/r^2)$ for mean $\langle\beta_e\rangle = \langle\beta_\infty\rangle = +0.2$ (red), 0 (black) and -0.2 (blue) and $0 < r_1/R_e < r_2/R_e < 1$.

3.2 Varying anisotropy

For $\beta_{\text{dOM}}(r) = \beta_1/(1 + r_1^2/r^2) + \beta_2/(1 + r_2^2/r^2)$ the radial mean for $0 \leq r \leq R_e$ β_e and the anisotropy at infinity $\beta_\infty = \beta_1 + \beta_2$ are assumed to be drawn from a Gaussian distribution with a standard deviation of 0.2. Because β_e can differ from β_∞ for a galaxy (although the means for the entire sample are assumed to be the same, i.e. $\langle\beta_e\rangle = \langle\beta_\infty\rangle$) and $0 < r_1/R_e < r_2/R_e < 1$ the adopted function allows wild variation within R_e . This does not necessarily mean that $\beta_{\text{dOM}}(r)$ represents or fully encompasses real behaviours of anisotropy. We just use $\beta_{\text{dOM}}(r)$ to mimic some uncertainties in varying anisotropies. Examples (taken from modelling results) of $\beta_{\text{dOM}}(r)$ for mean $\langle\beta_e\rangle = \langle\beta_\infty\rangle = +0.2$, 0 and -0.2 can be found in Fig. 6. Similar examples but with $\beta(r=0) \neq 0$ can be found in the appendix C of Chae et al. (2012).

Fig. 7 shows the predicted distributions of η for the same combinations of $(n, \langle\beta_e\rangle)$ as in Fig. 4 of the constant anisotropy case. Compared with the constant anisotropy case the predicted mean $\langle\eta\rangle$ shifts by ≈ -0.01 for the same input of $(n, \langle\beta\rangle)$. Consequently, the empirical value of η is best matched by the case $n = 1$. The case $n = 2$ is now disfavoured. Interestingly, Bekenstein’s model can now be consistent with the empirical value with a suitable choice of $\langle\beta_e\rangle$ although it may not be a preferred model. These results confirm that anisotropy shapes can matter in the study of MOND (as well as DM) in spheroidal galaxies.

The width (containing 68 percent) of the distribution (~ 0.27) is about 20 percent larger compared with the constant anisotropy case, but still somewhat lower than the measured standard deviation. However, the marginal discrepancy may be a result of non-Gaussian nature of the distribution. Indeed, the standard deviation of the distribution (~ 0.4) is larger than the 68 percent width and matches well the measured standard deviation.

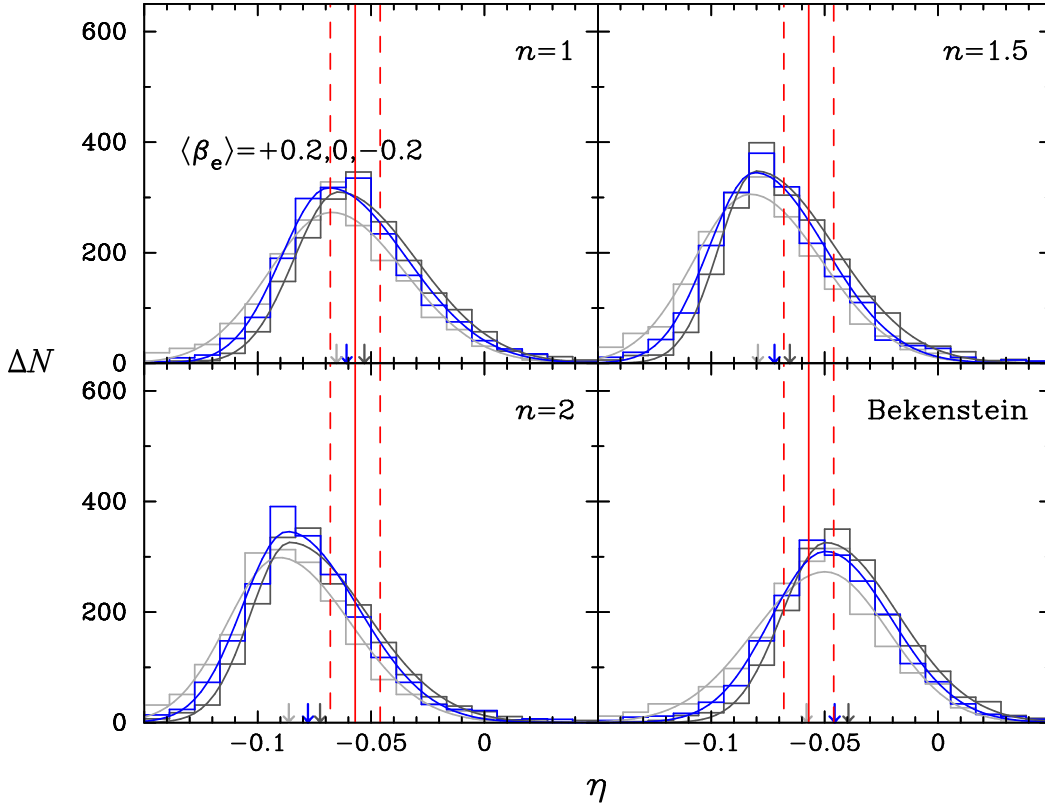


Figure 7. Same as Fig. 4 except that radially varying anisotropies are used and β_e refers to the radial average of an anisotropy within R_e of a galaxy.

4 DISCUSSION AND CONCLUSIONS

We have investigated VDPs for $r \lesssim R_e$ of ~ 2000 nearly round SDSS galaxies with $10 \lesssim \log_{10}(M_*/M_\odot) \lesssim 12$ (mean ≈ 11.3). Previous study by Chae et al. (2014) shows that the predicted distribution of VDP slope η (equation 13) cannot match an observed distribution without DM under Newtonian gravity (see also Fig. 3). Furthermore, as shown in Chae et al. (2014) each galaxy requires different amount and profile of DM. DM fraction within R_e ranges from $f_{\text{DM}} \approx 0.1 - 0.5$ (68% range: see Fig. 2) and the inner DM density profile slope α , in the generalised Navarro-Frenk-White (Navarro, Frenk & White 1997) parameterisation $\rho_{\text{DM}}(r) \propto (r/r_s)^{-\alpha}(1+r/r_s)^{-3+\alpha}$, ranges from $\alpha \approx 0.7 - 1.5$ (68%). These results mean that elliptical galaxies do require DM under Newtonian gravity in a statistical sense, although some fraction of galaxies may not contain significant amount in the optical region.

Our analysis of the same galaxies under MOND here indicates that the observationally-derived value of η (in 11 nearly round ATLAS^{3D} galaxies) can be reproduced based on a single MOND interpolating function without DM applied to all the galaxies. It is particularly striking that with an interpolation function similar to that of $n = 1$ or 2 in equation (5), used in various MOND studies particularly for disc galaxies (e.g. Famaey & Binney 2005; Sanders & Noordermeer 2007; Angus et al. 2008; Milgrom 2012), the empirical η value can be easily matched with a relaxed assumption of VD anisotropy (Figs. 4 and 7).

The specific functional form of MOND interpolating function depends, however, on the assumption on VD anisotropy (Figs. 4 and 7) and cannot be uniquely determined from the current empirical η value. The implied interpolating function can be varied by varying mean anisotropy or radial behaviours. For constant anisotropy and the functional form given by equation (5), mean anisotropy $\langle\beta\rangle = +0.2, 0$ and -0.2 give, respectively, $0.7 \lesssim n \lesssim 1.4$, $1.1 \lesssim n \lesssim 1.9$ and $1.3 \lesssim n \lesssim 2.5$. For the case of radially varying anisotropy there is an overall shift of $\Delta n \approx -0.5$ for the same value of mean anisotropy so that the traditionally standard model $n = 2$ is disfavoured. These manifest a degeneracy between MOND interpolating function and VD anisotropy, which is reminiscent of the well-known mass-anisotropy degeneracy under standard dynamics (e.g. Binney & Mamon 1982). This interpolating function-anisotropy degeneracy can be alleviated by a more precise empirical value of $\langle\eta\rangle$ or prior constraints on anisotropy.

Our analysis has been limited to nearly round galaxies (under the spherical symmetry assumption) in the intermediate acceleration regime although they cover a broad range of mass and size. A MOND analysis of ETGs of any ellipticity is considerably more challenging but would be necessary for a more rigorous test of MOND in spheroidal systems. If a random sample of elliptical galaxies (drawn from the same SDSS parent sample of ETGs using the same criteria except for the ellipticity limit) is analysed based on the MOND spherical Jeans equation (equation 2), the result-

ing η -distribution has a similar mean but a somewhat larger scatter, probably hinting that MOND works also for ETGs of any ellipticity.

Our analysis provides a novel and rigorous test of MOND in spheroidal galaxies in the sense that it is based on a statistically representative sample of spheroidal galaxies and a range of possibilities of VD anisotropy. Our test is most sensitive at $r \lesssim R_e/2$ where gravitational acceleration g due to the baryonic mass distribution is $\gtrsim a_0$ (Fig. 8). However, our galaxies cover the range $0.1R_e \lesssim r \lesssim R_e$ (see Fig. 1 of Chae et al. 2014) for which $0.3a_0 \lesssim g \lesssim 100a_0$ (Fig. 8). Our results support the view that MOND suggested by dynamics of rotating galaxies is also likely to be valid for dispersion-supported galaxies in their inner regions ($r \lesssim R_e$). Our results are in line with the test of MOND through hydrostatic equilibrium in two X-ray bright elliptical galaxies over a wide acceleration range by Milgrom (2012).

In this work we could not separately consider slow and fast rotators because the necessary kinematic information is not available for the analysed SDSS galaxies. The fact that the similarly selected ATLAS^{3D} elliptical galaxies are nearly evenly divided (see section 2) hints that the SDSS sample may also contain both kinematic classes, although it is likely to be somewhat biased towards slow rotators as the galaxies are on average more massive and larger than the ATLAS^{3D} counterparts (see Fig. 2). Recently, Samurović (2014) carried out individual Jeans modelling of ten elliptical galaxies, four of whom are slow rotators, based on observed GC kinematic data up to several effective radii. Considering two cases of constant anisotropy $\beta = 0, -0.2$ and one case of radially varying $\beta(r) \approx 0.5r/(r + 1.4R_e)$ for MOND interpolating functions of $n = 1, 2$ in equation (5) and that of equation (7), Samurović (2014) could not find successful fits of slow rotators without additional component of DM beyond $\sim 2\text{--}3R_e$. For one galaxy NGC 4486 (M87), which is in the central region of a cluster, the considered MOND models and anisotropies had difficulty of fitting GC kinematic data even in the inner region ($r \lesssim 0.5R_e$). However, as Samurović (2014) notes, it remains unclear whether these problems based on limited cases of anisotropies imply breakdown of MOND for certain objects. In this work we have considered a broader range of possibilities of anisotropy and found that VDPs of a mixed population of fast and slow rotators for $r \lesssim R_e$ could be statistically explained by MOND without any DM.

If the empirical MOND law is to be truly meaningful, there must exist a universal interpolating function. Studies up to the present indicate that this is a reasonable possibility. However, a firm conclusion can only be reached through precise determination of interpolating functions of galaxies of various types. Our analysis shows that the statistics of VDPs of elliptical galaxies provides a useful tool to test interpolating functions. This statistical analysis can complement individual analyses that can be performed with detailed kinematic data (e.g. Samurović 2014). Despite its current limits, our analysis appears to support the simple interpolating function [equation (5) with $n = 1$] (see Figs. 4 and 7), which has also been preferred by galaxy rotation data (e.g. Famaey & Binney 2005; Sanders & Noordermeer 2007) and studies of elliptical galaxies [see Milgrom (2012) and references therein], although we cannot yet rule out the

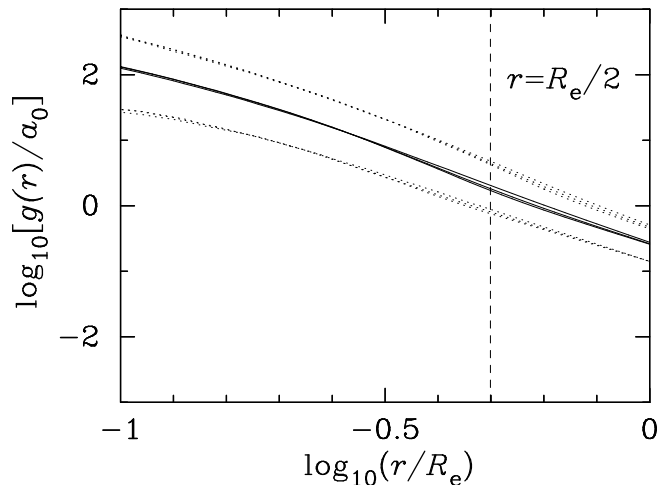


Figure 8. Distribution of gravitational acceleration $g(r)$ normalised by $a_0 = 1.2 \times 10^{-10} \text{ m s}^{-2}$ due to stellar mass within radius r in ~ 2000 nearly round SDSS galaxies based on modelling results with $n = 1, 1.5$ and 2 for $\langle\beta\rangle = 0$ shown in Fig. 4. The solid curves represent the medians while the dotted curves represent the 95% limits. The observed VDs of SDSS galaxies analysed in this work are luminosity-weighted LOSVDs within projected radius R_{ap} , which is peaked at $R_e/2$ (represented by the vertical dashed line) but ranges from $\sim 0.1R_e$ up to $\sim R_e$.

traditionally standard model with $n = 2$ or even the interpolating function (equation 7) implied by Bekenstein’s modified gravity (Bekenstein 2004; Zhao & Famaey 2006).

If a single interpolating function turns out to explain dynamics of all galaxies, that would have far-reaching implications. In this respect it would be quite interesting to empirically verify and determine the supposed universal MOND interpolating function with future data. For spheroidal galaxies both statistical (for large samples, as was demonstrated in this study) and individual (for large radial extent, performed earlier and ongoing) analyses of VDPs will be useful.

We are grateful to Srdjan Samurović for providing a thorough and helpful report of the submitted manuscript. We also thank Maurice van Putten for useful discussions/comments and Mariangela Bernardi for helpful communication regarding SDSS galaxies.

REFERENCES

- Ade P. A. R., et al. (Planck Collaboration), 2014, A&A, 571, A16
- Angus G. W., Famaey B., Tiret O., Combes F., Zhao H. S., 2008, MNRAS, 383, L1
- Bekenstein J. D., 2004, Phys. Rev. D, 70, 083509
- Bernardi M., Shankar F., Hyde J. B., Mei S., Marulli F., Sheth R. K., 2010, MNRAS, 404, 2087
- Bertone G., Hooper D., Silk J., 2005, Phys. Rep., 405, 279
- Binney J., Mamon G. A., 1982, MNRAS, 200, 361
- Cappellari M., et al., 2006, MNRAS, 366, 1126
- Cappellari M., et al., 2007, MNRAS, 379, 418
- Cappellari M., et al., 2011, MNRAS, 413, 813

- Cappellari M., et al., 2013a, MNRAS, 432, 1709
 Cappellari M., et al., 2013b, MNRAS, 432, 1862
 Chabrier G., 2003, ApJ, 586, L133
 Chae K.-H., 2014, ApJ, 788, L15
 Chae K.-H., Bernardi M., Kravtsov A. V., 2014, MNRAS, 437, 3670
 Chae K.-H., Kravtsov A. V., Frieman J. A., Bernardi M., 2012, JCAP, 11, 004
 Chiu M.-C., Ko C. M., Tian Y., Zhao H., 2011, Phys. Rev. D, 83, 063523
 Conroy C., van Dokkum P. G., 2012, ApJ, 760, 71
 Dekel A., Stoehr F., Mamon G. A., Cox T. J., Novak G. S., Primack J. R., 2005, Nature, 437, 707
 Emsellem E., et al., 2007, MNRAS, 379, 401
 Emsellem E., et al., 2011, MNRAS, 414, 888
 Famaey B., Binney J., 2005, MNRAS, 363, 603
 Famaey B., Bruneton J. P., Zhao H., 2007, MNRAS, 377, L79
 Famaey B., McGaugh S. S., 2012, Living Reviews in Relativity, 15, 10
 Ferreras I., Mavromatos N. E., Sakellariadou M., Yusaf M. F., 2012, Phys. Rev. D, 86, 083507
 Gerhard O., Kronawitter A., Saglia R. P., Bender R., 2001, AJ, 121, 1936
 Hinshaw G., et al., 2013, ApJS, 208, 19
 Klypin A., Prada F., 2009, ApJ, 690, 1488
 Kroupa P., Pawlowski M., Milgrom M., 2012, Int. J. Mod. Phys. D, 21, 1230003
 McGaugh S. S., 2004, ApJ, 609, 652
 McGaugh S. S., 2005, ApJ, 632, 859
 McGaugh S. S., 2011, Phys. Rev. Lett., 106, 121303
 McGaugh S. S., 2014, arXiv:1404.7525
 Meert A., Vikram V., Bernardi M., 2013, MNRAS, 433, 1344
 Meert A., Vikram V., Bernardi M., 2015, MNRAS, 446, 3943
 Milgrom M., 1983, ApJ, 270, 365
 Milgrom M., 2012, Phys. Rev. Lett., 109, 131101
 Milgrom M., Sanders R. H., 2003, ApJ, 599, L25
 Milgrom M., Sanders R. H., 2008, ApJ, 678, 131
 Mo H., van den Bosch F., White S., 2010, Galaxy Formation and Evolution, Cambridge Univ. Press, Cambridge, UK
 Navarro J. F., Frenk C. S., White S. D. M., 1997, ApJ, 490, 493
 Prugniel P., Simien F., 1997, A&A, 321, 111
 Richtler T., Schuberth Y., Hilker M., Dirsch B., Bassino L., Romanowsky A. J., 2008, A&A, 478, L23
 Richtler T., Famaey B., Gentile G., Schuberth Y., 2011, A&A, 531, A100
 Salinas R., Richtler T., Bassino L. P., Romanowsky A. J., Schuberth Y., 2012, A&A, 538, A87
 Salpeter E. E., 1955, ApJ, 121, 161
 Samurović S., 2010, A&A, 514, A95
 Samurović S., 2012, A&A, 541, A138
 Samurović S., 2014, A&A, 570, A132
 Samurović S., Ćirković M. M., 2008, A&A, 488, 873
 Sancisi R., 2004, IAU Symposium No. 220, p.233
 Sanders R. H., 2014a, The Dark Matter Problem, Cambridge Univ. Press, Cambridge, UK
 Sanders R. H., 2014b, MNRAS, 439, 1781
 Sanders R. H., Noordermeer E., 2007, MNRAS, 379, 702
 Schuberth Y., Richtler T., Hilker M., Salinas R., Dirsch B., Larsen S. S., 2012, A&A, 544, A115
 Scott N., et al., 2013, MNRAS, 432, 1894
 Sérsic J. L., 1968, Atlas de Galaxias Australes, Observatorio Astronómico de Córdoba
 Thomas J., Saglia R. P., Bender R., Thomas D., Gebhardt K., Magorrian J., Corsini E. M., Wegner G., 2007, MNRAS, 382, 657
 Tiret O., Combes F., Angus G. W., Famaey B., Zhao H. S., 2007, A&A, 476, L1
 Tortora C., Romanowsky A. J., Napolitano N. R., 2013, ApJ, 765, 8
 Trimble V., 1987, ARA&A, 25, 425
 York D. G., et al., 2000, AJ, 120, 1579
 Zhao H. S., Famaey B., 2006, ApJ, 638, L9